2022

Homework Report

CONTROL IN ROBOTICS COURSE

FATEMEH HEIRAN

ISFAHAN UNIVERSITY | Isfahan - Iran

Contents

The Robot Model

3-Dof Articulated Robot Structure

In an articulated robot, joints are all revolute, similar to a human's arm. They are the most common configuration for industrial robots. The selected articulated robot is the same as PUMA's robot first part which yields to the robot end effector position (simplified PUMA). The robot configuration is showed in right side of fig. 1. Accordingly, the robot consist of three revolute joint which implied 3 Dof in task space.

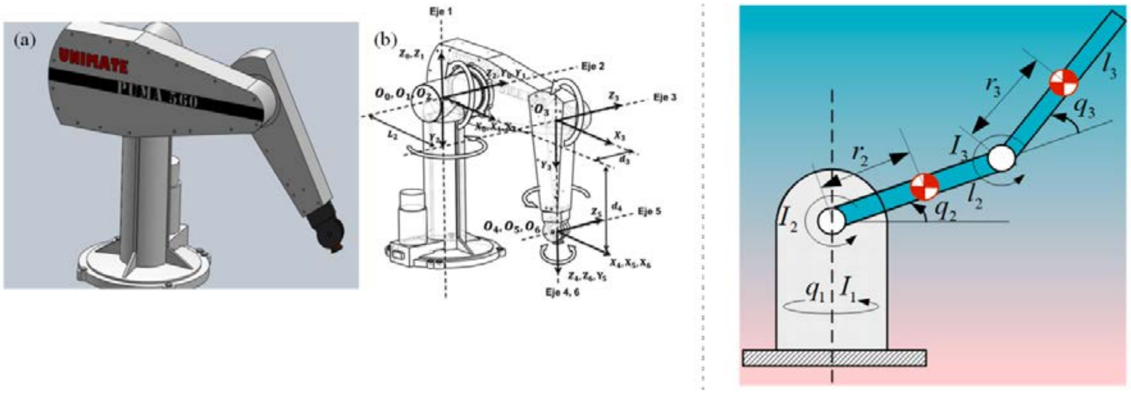

Figure 1- the left side picture is PUMA robot and the right side picture is the simplified PUMA robot [1]

Direct Kinematics

If we state the end effector coordinates of manipulator based on the angles of the joints, it means the forward kinematics. In other word, in forward kinematics, the measures of the joint space are available and we want to determine the measures of coordinate space. In reality, forward kinematics analyzing is a mapping from joint space to the coordinate space. The direct kinematics of this robot comes as follows [2]:

$$P_x = (l_2 \cos\theta_2 + l_3 \cos(\theta_2 + \theta_3)) * \sin\theta_1 \tag{1}$$

$$P_y = (l_2 \cos\theta_2 + l_3 \cos(\theta_2 + \theta_3)) * \cos\theta_1 \tag{2}$$

$$P_z = l_2 \sin\theta_2 + l_3 \sin(\theta_2 + \theta_3) + l_1 \tag{3}$$

Jacobian Matrix

The Jacobian matrix concluded from velocity analysis for the robot and is defined as [2]:

$$\dot{x} = \begin{bmatrix} C_1(l_3C_{23} + l_2C_2) & -S_1(l_3S_{23} + l_2S_2) & -l_3S_{23}S_1 \\ -S_1(l_3C_{23} + l_2C_2) & -C_1(l_3S_{23} + l_2S_2) & -l_3S_{23}C_1 \\ 0 & l_3C_{23} + l_2C_2 & l_3C_{23} \end{bmatrix} \dot{\theta} = J\dot{\theta} \tag{4}$$

Also in some analysis the derivative of Jacobian is needed, therefore it defined as:

$$j_{11} = -S_1\dot{\theta}_1(l_3C_{23} + l_2C_2) + C_1(-l_3S_{23}(\dot{\theta}_2 + \dot{\theta}_3) - l_2S_2\dot{\theta}_2) \tag{5}$$

$$j_{12} = -C_1\dot{\theta}_1(l_3S_{23} + l_2S_2) - S_1(l_3C_{23}(\dot{\theta}_2 + \dot{\theta}_3) + l_2C_2\dot{\theta}_2) \tag{6}$$

$$j_{13} = -l_3C_{23}(\dot{\theta}_2 + \dot{\theta}_3)S_1 - l_3S_{23}C_1\dot{\theta}_1 \tag{7}$$

$$j_{21} = -C_1\dot{\theta}_1(l_3C_{23} + l_2C_2) - S_1(-l_3S_{23}(\dot{\theta}_2 + \dot{\theta}_3) - l_2S_2\dot{\theta}_2) \tag{8}$$

$$j_{22} = S_1\dot{\theta}_1(l_3S_{23} + l_2S_2) - C_1(l_3C_{23}(\dot{\theta}_2 + \dot{\theta}_3) + l_2C_2\dot{\theta}_2) \tag{9}$$

$$j_{23} = -l_3C_{23}(\dot{\theta}_2 + \dot{\theta}_3)C_1 + l_3S_{23}S_1\dot{\theta}_1 \tag{10}$$

$$j_{31} = 0 \tag{11}$$

$$j_{32} = -l_3S_{23}(\dot{\theta}_2 + \dot{\theta}_3)C_1 - l_2S_2\dot{\theta}_2 \tag{12}$$

$$j_{33} = -l_3S_{23}(\dot{\theta}_2 + \dot{\theta}_3) \tag{13}$$

Direct Dynamics

According to [1], in the simplified PUMA560, m_1, m_2, m_3 are the mass of the turntable, the boom and the arm, respectively. The mass of the turntable can be ignored, l_2, l_3 are the length of the boom and the length of the arm, respectively, r_2, r_3 are the distance from the center of mass of the boom to the axis of rotation and the distance from the center of mass of the arm to the axis of rotation. I_1, I_2, I_3 are the moment of inertia about the rotation of each axis. Let:

$$a_1{=}m_2r_2^2+m_3l_2^2,\ a_2{=}m_3r_3^2,\ a_3=m_3r_3l_2\ b_1{=}(m_2r_2+m_3l_2)g,\ b_2{=}m_3r_3g$$

Establishing the dynamic equation based on the D-H rule:

$$M(\boldsymbol{q})\ddot{\boldsymbol{q}}+b(\boldsymbol{q},\dot{\boldsymbol{q}})\dot{\boldsymbol{q}}+f(\boldsymbol{q})=\boldsymbol{\tau} \tag{14}$$

Where,

$$M(\boldsymbol{q})=\begin{bmatrix} m_{11} & m_{12} & m_{13} \\ m_{21} & m_{22} & m_{23} \\ m_{31} & m_{32} & m_{33} \end{bmatrix} b(\boldsymbol{\theta},\dot{\boldsymbol{\theta}})=\begin{bmatrix} b_{11} & b_{12} & b_{13} \\ b_{21} & b_{22} & b_{23} \\ b_{31} & b_{32} & b_{33} \end{bmatrix} f(\boldsymbol{q})=\begin{bmatrix} 0 \\ b_1\cos q_2+b_2\cos(q_2+q_3) \\ b_2\cos(q_2+q_3) \end{bmatrix}$$

$$m_{11} = a_1 \cos^2 q_2 + a_2 \cos^2\left(q_2 + q_3\right) + 2a_3 \cos q_2 \cos\left(q_2 + q_3\right) + I_1,\ m_{22} = a_1 + a_2 + 2a_3 \cos q_3 + I_2$$

$$m_{33} = a_2 + I_3,\ m_{23} = m_{32} = a_2 + a_3 \cos q_3,\ m_{12} = m_{21} = m_{13} = m_{31} = 0$$

$$b_{11} = -\frac{1}{2} a_1 \dot{q}_2 \sin(2q_2) - \frac{1}{2} a_2 \left(\dot{q}_2 + \dot{q}_3\right) \sin(2q_2 + 2q_3) - a_3 \dot{q}_2 \sin(2q_2 + q_3) - \ a_3 \dot{q}_3 \cos q_2 \sin\left(q_2 + q_3\right)$$

$$b_{12} = -\frac{1}{2} a_1 \dot{q}_1 \sin(2q_2) - \frac{1}{2} a_2 \dot{q}_1 \sin(2q_2 + 2q_3) - a_3 \dot{q}_1 \sin(2q_2 + q_3)$$

$$b_{13} = -\frac{1}{2} a_2 \dot{q}_1 \sin(2q_2 + 2q_3) - a_3 \dot{q}_1 \cos q_2 \sin(q_2 + q_3),\ b_{21} = -b_{12},\ b_{22} = -a_3 \dot{q}_3 \sin q_3,$$

$$b_{23} = -a_3 (\dot{q}_2 + \dot{q}_3) \sin q_3,\ b_{31} = -b_{13},\ b_{32} = a_3 \dot{q}_2 \sin q_3,\ b_{33} = 0$$

Regressor Matrix

```
M = [cos(q(2))^2*ddq(1), cos(q(2) + q(3))^2*ddq(1), 2*cos(q(2))*cos(q(2) +
q(3))*ddq(1), ddq(1), 0, 0, 0, 0, 0;...
    ddq(2), ddq(2) + ddq(3), 2*cos(q(3))*ddq(2) + ddq(3)*cos(q(3)), 0, ddq(2),
0, 0, 0, 0;...
    0, ddq(2) + ddq(3), ddq(2)*cos(q(3)), 0, 0, ddq(3), 0, 0, 0];

C = [-0.5*dq(2)*sin(2*q(2))*dq(1) - 0.5*dq(2)*dq(1)*sin(2*q(2)), - 0.5*(dq(2) +
dq(3))*sin(2*q(2) + 2*q(3))*dq(1)...
    - 0.5*dq(2)*dq(1)*sin(2*q(2) + 2*q(3)) - 0.5*dq(3)*dq(1)*sin(2*q(2) +
2*q(3)), - dq(2)*sin(2*q(2) + q(3))*dq(1)...
    - dq(1)*dq(3)*cos(q(2))*sin(q(2) + q(3)) - dq(2)*dq(1)*sin(2*q(2) + q(3)) -
dq(3)*dq(1)*cos(q(2))*sin(q(2) + q(3))...
    , 0, 0, 0, 0, 0, 0;...
    0.5*dq(1)*dq(1)*sin(2*q(2)), 0.5*dq(1)*dq(1)*sin(2*q(2) + 2*q(3)),
dq(1)*dq(1)*sin(2*q(2) + q(3)) - dq(2)*dq(3)...
    *sin(q(3)) - dq(3)*(dq(2) + dq(3))*sin(q(3)), 0, 0, 0, 0, 0, 0;...
    0, 0.5*dq(1)*dq(1)*sin(2*q(2) + 2*q(3)), dq(1)*dq(1)*cos(q(2))*sin(q(2) +
q(3)) + dq(2)*dq(2)*sin(q(3)),...
    0, 0, 0, 0, 0, 0];

G = [0, 0, 0, 0, 0, 0, 0, 0, 0; ...
    0, 0, 0, 0, 0, 0, sin(q(2))*g/2, - sin(q(2) + q(3))*g/2, - sin(q(2))*g; ...
    0, 0, 0, 0, 0, 0, 0, -sin(q(2) + q(3))*g/2, 0];

Y = M + C + G;
```

Parameters Vector

```
theta = [a1; a2; a3; I1; I2; I3; m2*l2; m3*l3; m3*l2]
```

Controller Design and Simulation

Trajectory Planning

The trajectory planning for the robot joint angles has been take place with assuming the initial and final position, velocity and acceleration between time 0 to 5 second as follows.

$$x_1 = \begin{bmatrix}\theta_{1i} & \dot{\theta}_{1i} & \ddot{\theta}_{1i} & \theta_{1f} & \dot{\theta}_{1f} & \ddot{\theta}_{1f}\end{bmatrix} = [0, 0, pi/12, 2pi/3, 0, 0]$$

$$x_2 = \begin{bmatrix}\theta_{2i} & \dot{\theta}_{2i} & \ddot{\theta}_{2i} & \theta_{2f} & \dot{\theta}_{2f} & \ddot{\theta}_{2f}\end{bmatrix} = [0, 0, pi/12, pi/3, 0, 0]$$

$$x_3 = \begin{bmatrix}\theta_{3i} & \dot{\theta}_{3i} & \ddot{\theta}_{3i} & \theta_{3f} & \dot{\theta}_{3f} & \ddot{\theta}_{3f}\end{bmatrix} = [0, 0, pi/12, 5pi/6, 0, 0]$$

Which yields to the trajectory planning as follows:

```
theta1 = 0.1309*t^2 + 0.0147*t^3 - 0.0085*t^4 + 0.0007*t^5;
theta2 = 0.1309*t^2 - 0.0188*t^3 - 0.001*t^4 + 0.0002*t^5;
theta3 = 0.1309*t^2 + 0.0314*t^3 - 0.0123*t^4 + 0.001*t^5;
```

- *Hint 1: there is a m file named trajectoryPlanning to obtain the trajectory.*
- *Hint 2: in the case of impedance and parallel control because of singularity in above trajectory, the simulation doesn't work well. Therefore, we changed the trajectory as follows:*

  ```
  theta1 = 2*exp(-0.1*t);
  theta2 = 1 + exp(-0.15*t);
  theta3 = 0.5 + 2*exp(-0.2*t);
  ```

Assumptions

The robot parameters are considered as follows:

```
m1 = 1;
m2 = 1;
m3 = 1;

l1 = 1;
l2 = 1;
l3 = 1;

r1 = l1/2;
r2 = l2/2;
r3 = l3/2;

R1 = 0.05;
R2 = 0.05;
R3 = 0.05;

g = 9.81;
```

PD Controller

PD

In this controller the terms including gravity (g) were omitted. Fig. 2 show the controller designed in Simulink.

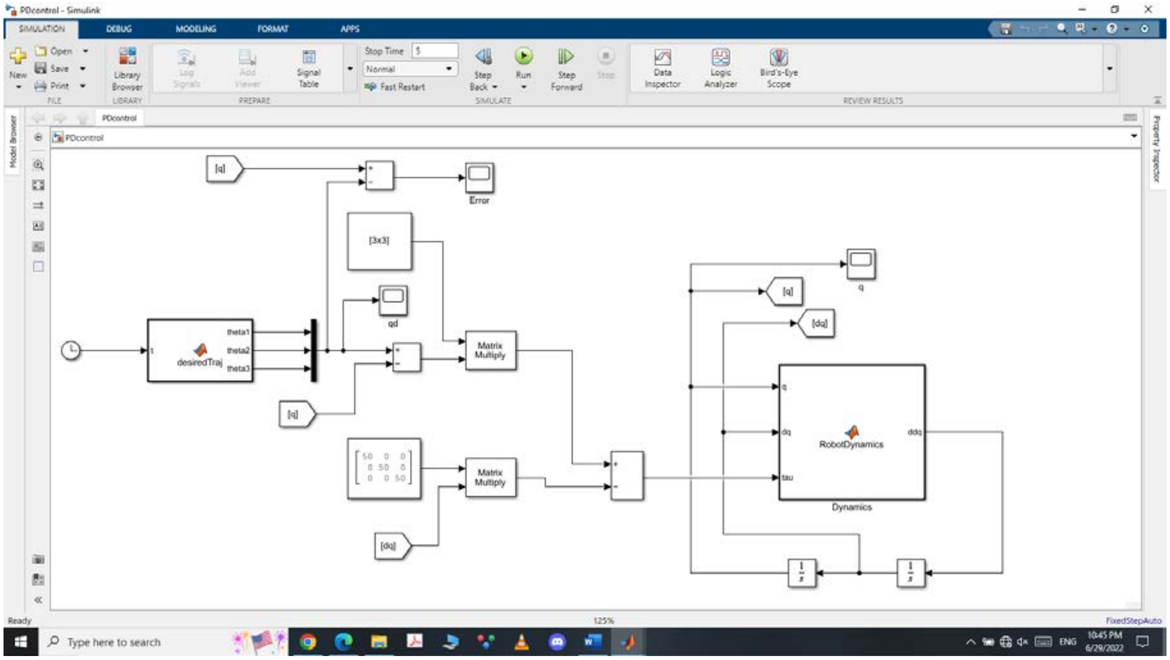

Stop Time 5

Normal

Figure 2- Simulation of PD Controller

According to the simulation, the error is revealed in fig. 3.

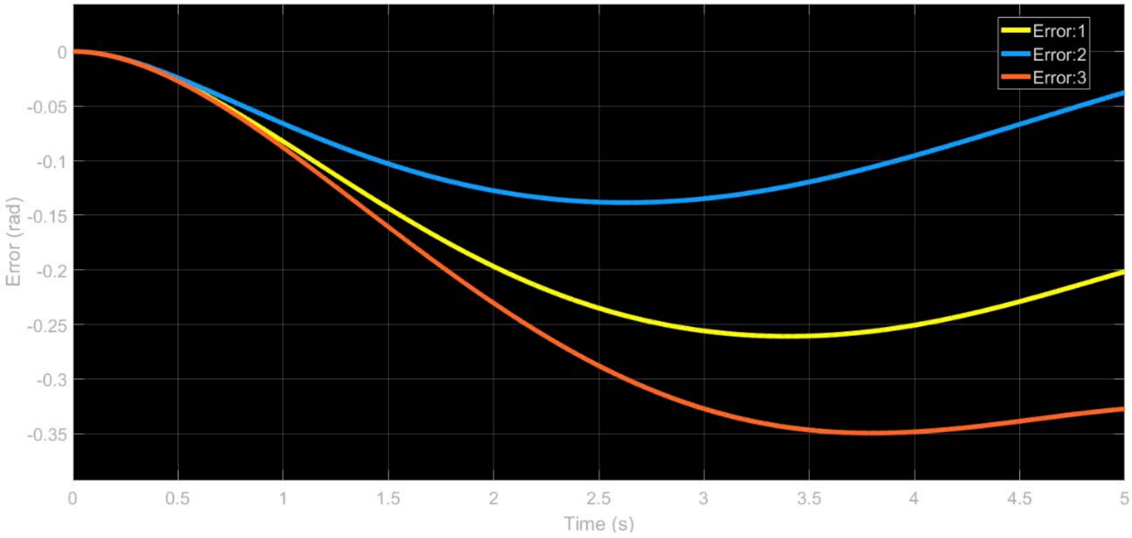

Figure 3- PD controller simulation results

PD + Gravity Controller

This controller is PD type with considering gravity in designing controller. Fig. 4 show the controller designed in Simulink.

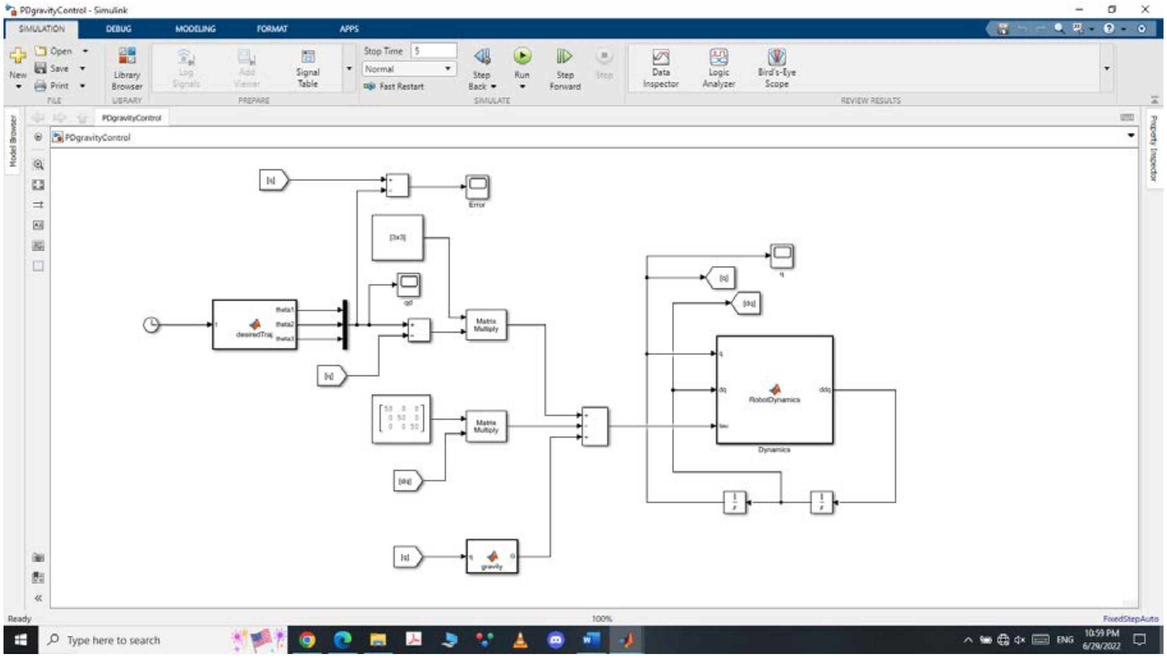

Figure 4- Simulation of PD + gravity Controller

According to the simulation, the error is revealed in fig. 5.

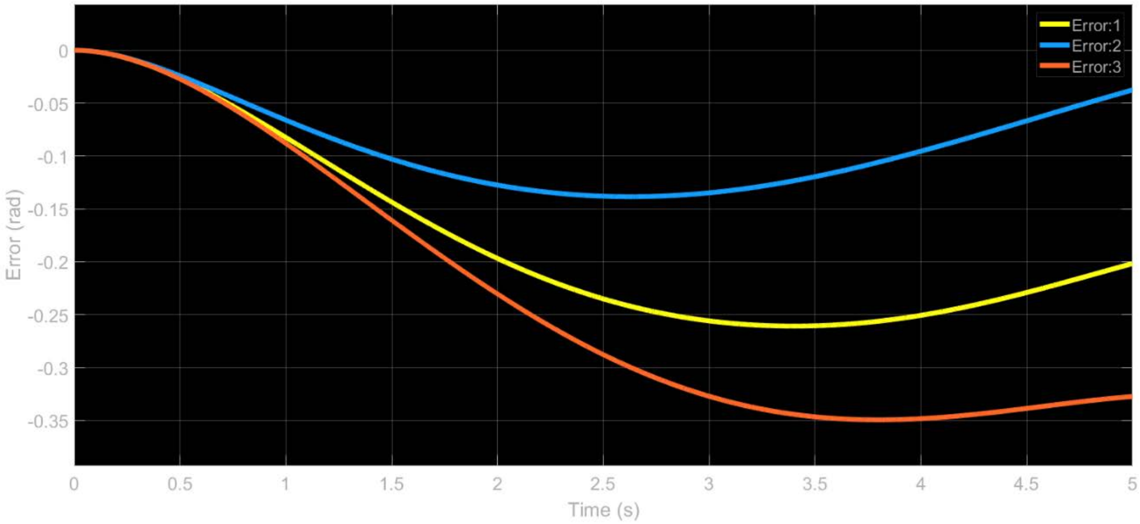

Figure 5- PD + gravity controller simulation results

Inverse Dynamics Control

PD Inverse Dynamics

The fig. 6 shows the simulations of the controller. The control design assumptions are defined as follows:

```
Kp = [1 0 0; 0 1 0; 0 0 1];
Kd = [1 0 0; 0 1 0; 0 0 1];
```

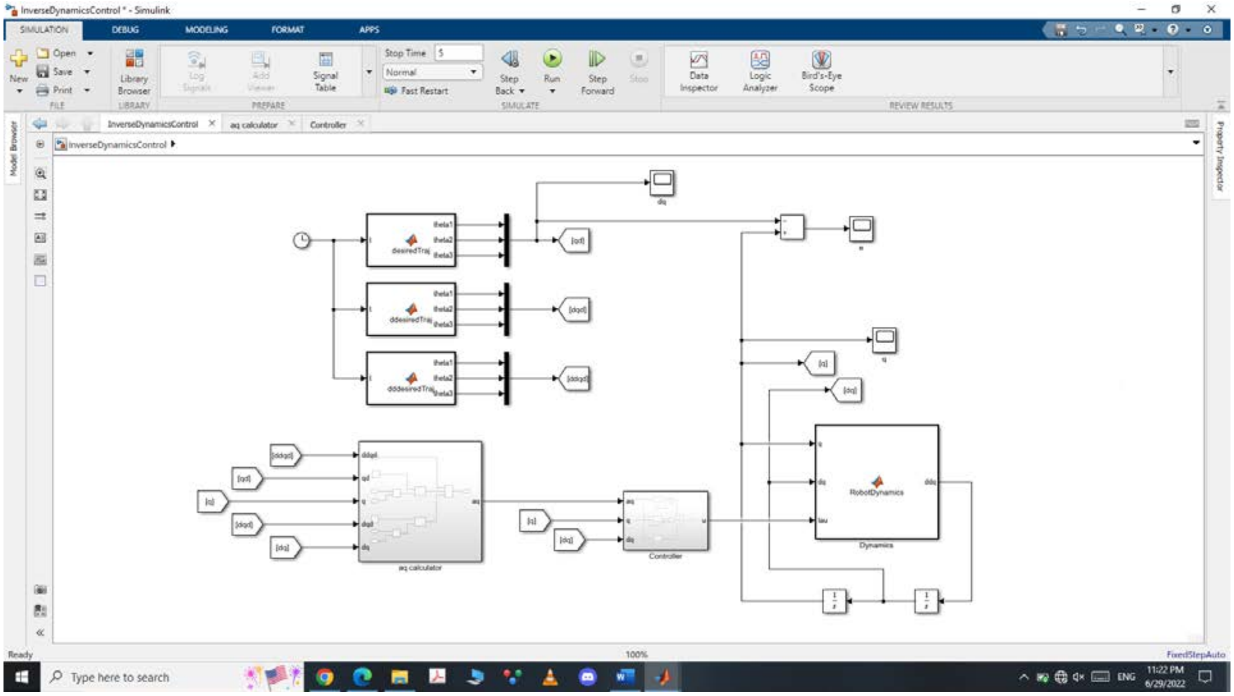

Figure 6- Simulation of PD inverse dynamics Controller

According to the simulation, the error is revealed in fig. 7.

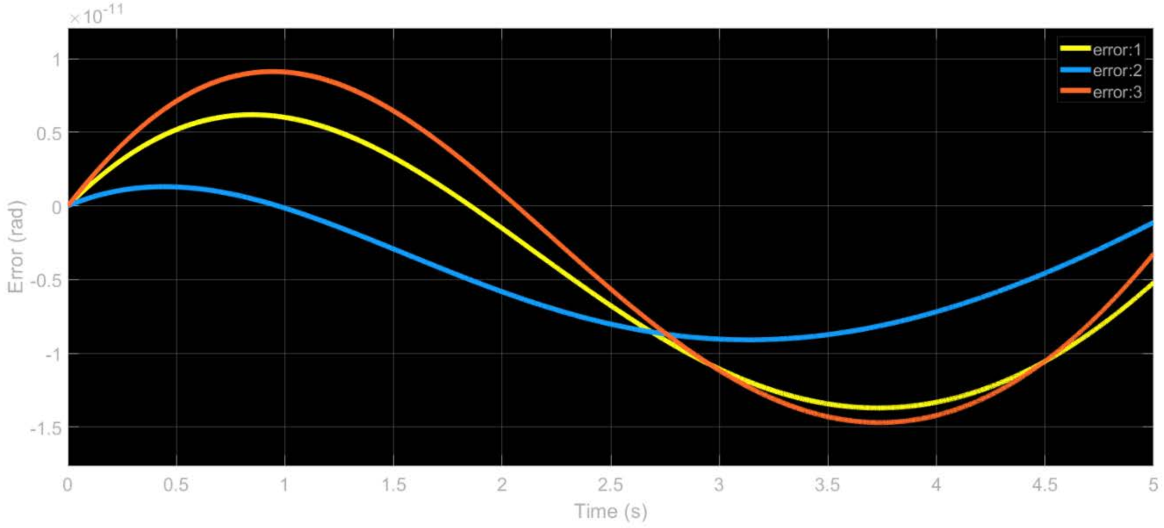

Figure 7- PD inverse dynamics controller simulation results

Robust Inverse Dynamics

The fig. 8 shows the simulations of the controller. The control design assumptions are defined as follows:

```
kd1 = 100; kd2 = 100; kd3 = 100;
kp1 = 100; kp2 = 100; kp3 = 100;
P = [-49 0 0 53 0 0; 0 -49 0 0 53 0; 0 0 -49 0 0 53; 53 0 0 -59 0 0; 0 53 0 0 -
59 0; 0 0 53 0 0 -59];
Rho = 0.01;
Mhat = [3.5 0 0; 0 3.5 0.75; 0 0.75 1.25];
Chat = [2 1.25 1; -1.25 0.5 0.5; -1 0.5 0];
Ghat = [0; 20; 5];
epsilon = 0.1;
```

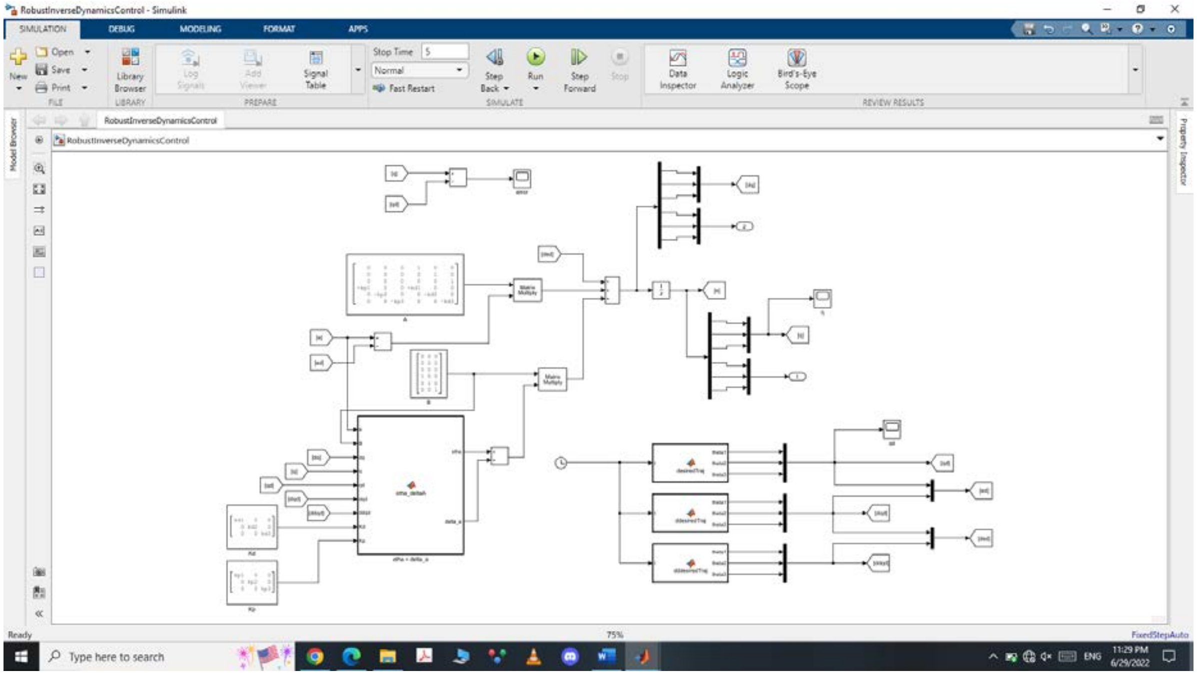

Figure 8- Simulation of robust inverse dynamics Controller

According to the simulation, the error is revealed in fig. 9.

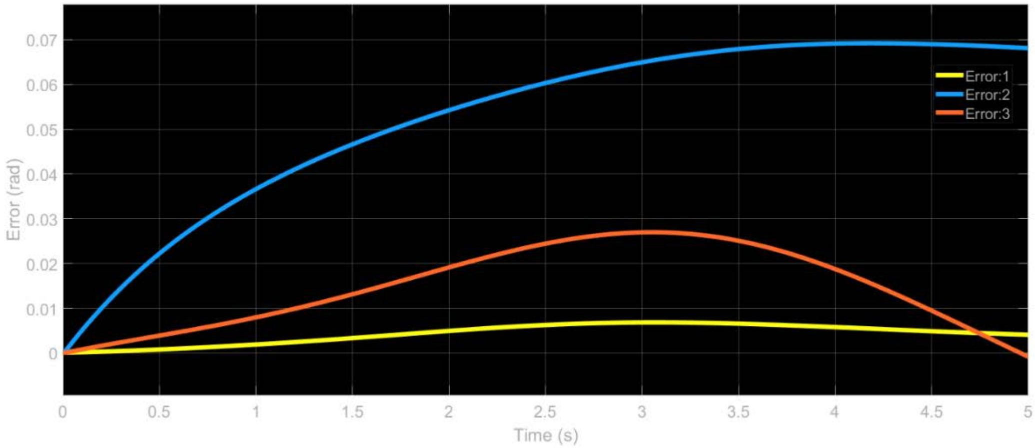

Figure 9- Robust inverse dynamics controller simulation results

Adaptive Inverse Dynamics

The fig. 10 shows the simulations of the controller. The control design assumptions are defined as follows:

```
gamma = 0.00001*[1 0 0 0 0 0 0 0 0; 0 1 0 0 0 0 0 0 0; 0 0 1 0 0 0 0 0 0; 0 0 0
1 0 0 0 0 0; 0 0 0 0 1 0 0 0 0; 0 0 0 0 0 1 0 0 0; 0 0 0 0 0 0 1 0 0; 0 0 0 0 0
0 0 1 0; 0 0 0 0 0 0 0 0 1];
P = [-49 0 0 53 0 0; 0 -49 0 0 53 0; 0 0 -49 0 0 53; 53 0 0 -59 0 0; 0 53 0 0 -
59 0; 0 0 53 0 0 -59];
kd1 = 60;
kd2 = 60;
kd3 = 60;
kp1 = 60;
kp2 = 60;
kp3 = 60;
Mhat = [3.5 0 0; 0 3.5 0.75; 0 0.75 1.25];
theta = [1.25; 0.25; 0.5; 1; 1; 1; 1; 1; 1];
```

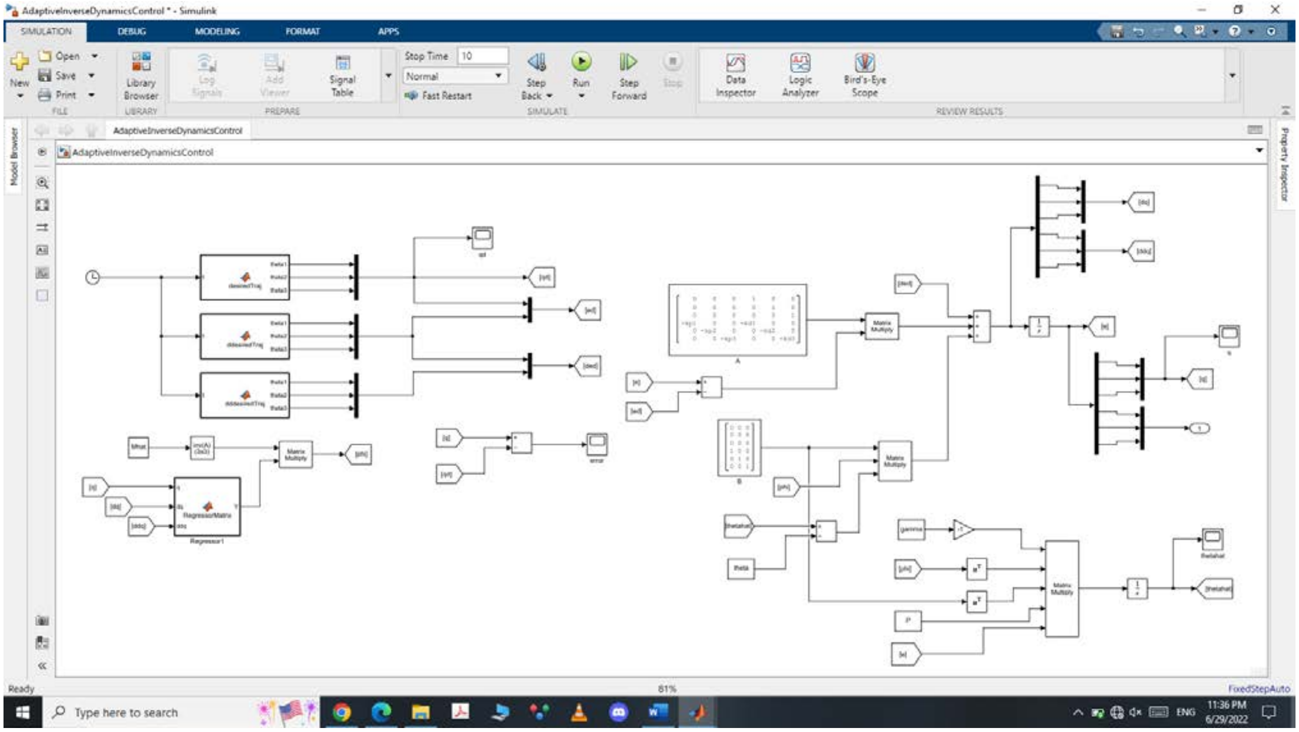

Figure 10- Simulation of adaptive inverse dynamics Controller

According to the simulation, the error is revealed in fig. 11.

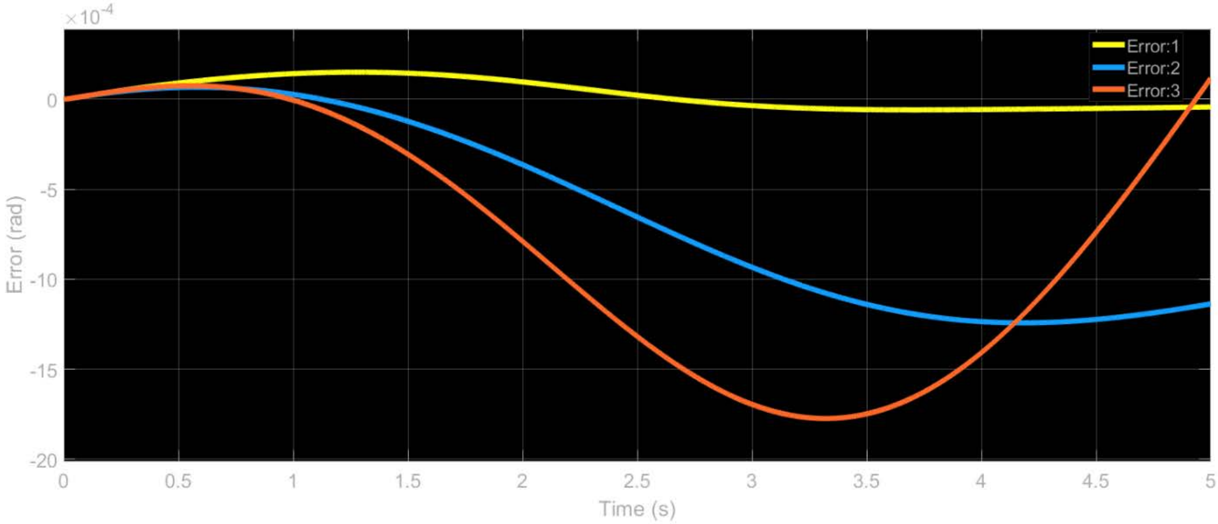

Figure 11- Adaptive inverse dynamics controller simulation results

Passivity Based Control

PD Passivity Based

The fig. 12 shows the simulations of the controller. The control design assumptions are defined as follows:

```
gamma = 0.1.*[1 0 0; 0 1 0; 0 0 1];
K = 0.01.*[1 1 1; 0 1 0; 0 0 1];
```

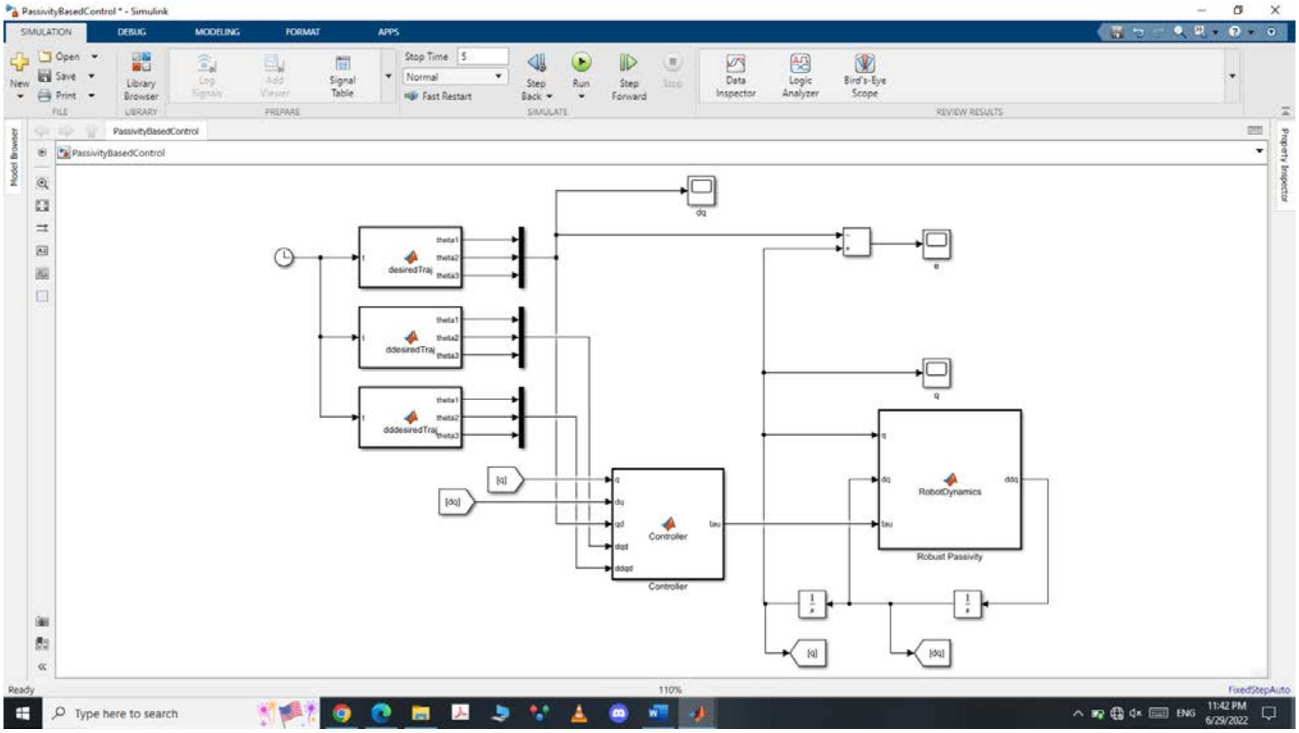

Figure 12- Simulation of PD passivity based Controller

According to the simulation, the error is revealed in fig. 13.

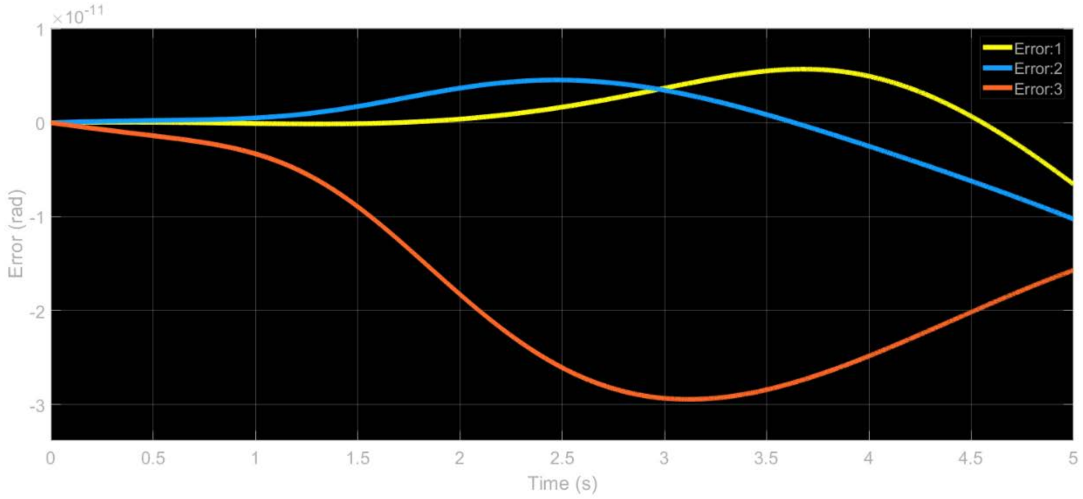

Figure 13- PD passivity based controller simulation results

Robust Passivity Based

The fig. 14 shows the simulations of the controller. The control design assumptions are defined as follows:

```
theta  = [1.25; 0.25; 0.5; 1; 1; 1; 1; 1; 1];
theta0 = theta.*3;
K = 100.*[1 0 0; 0 1 0; 0 0 1];
gamma = 1.*[1 0 0; 0 1 0; 0 0 1];
Rho = 10;
epsilon = 0.1;
```

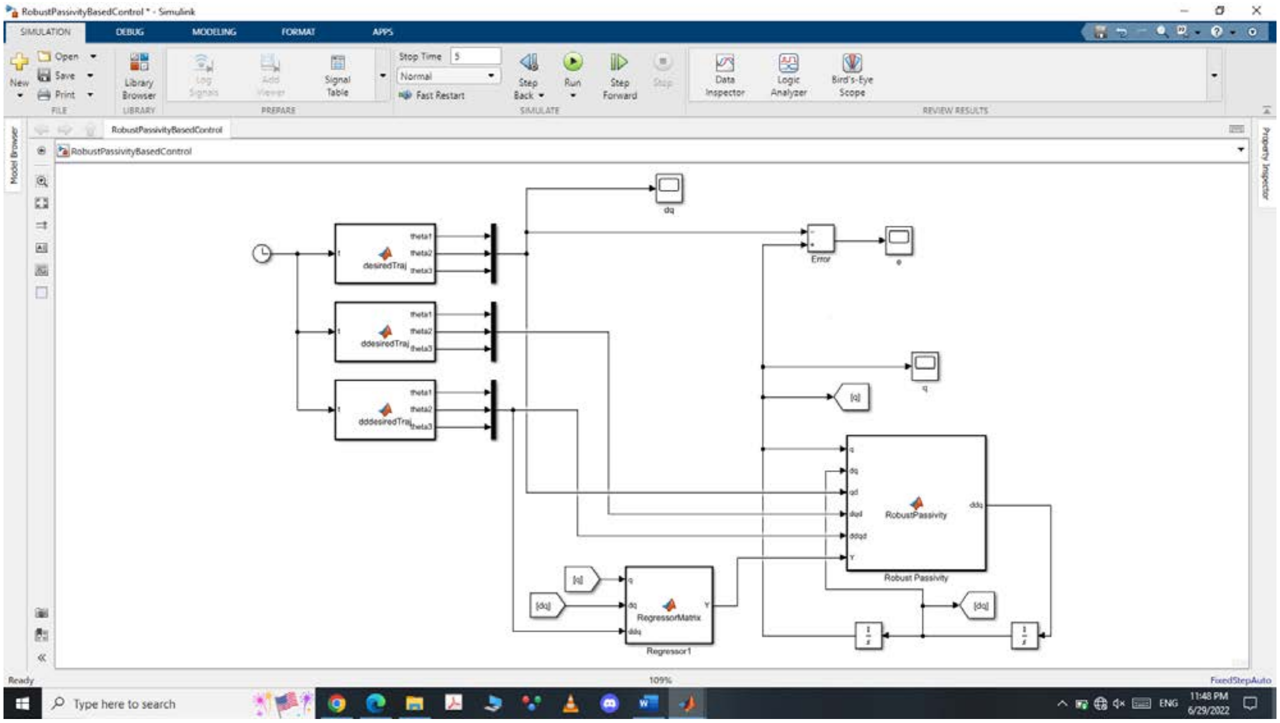

Figure 14- Simulation of robust passivity based Controller

According to the simulation, the error is revealed in fig. 15.

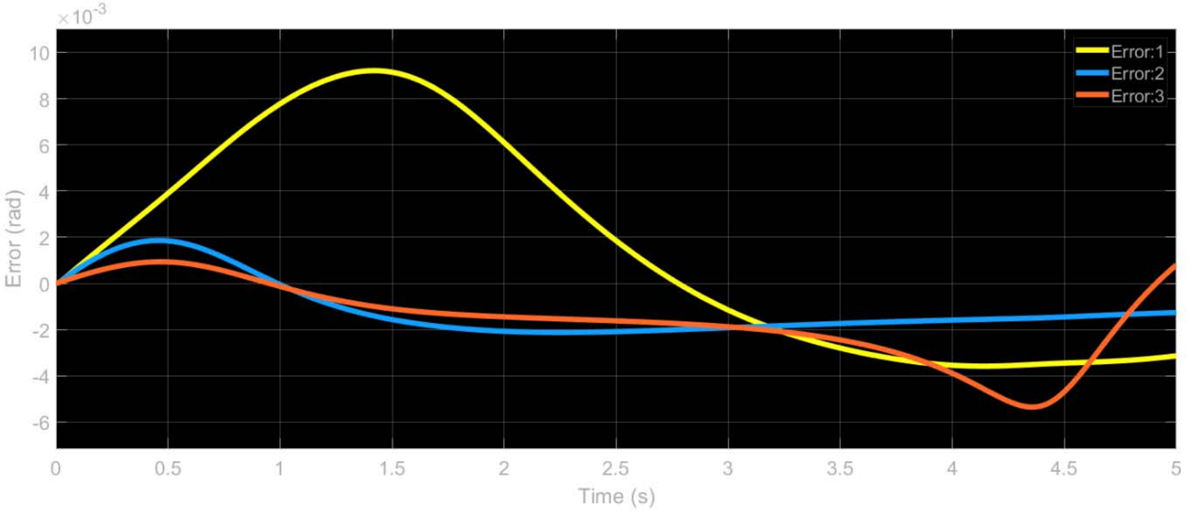

Figure 15- Robust passivity based controller simulation results

Adaptive Passivity Based

The fig. 16 shows the simulations of the controller. The control design assumptions are defined as follows:

```
K = 100.*[1 0 0; 0 1 0; 0 0 1];
gamma = 1.*[1 0 0; 0 1 0; 0 0 1];
theta  = [1.25; 0.25; 0.5; 1; 1; 1; 1; 1; 1];
```

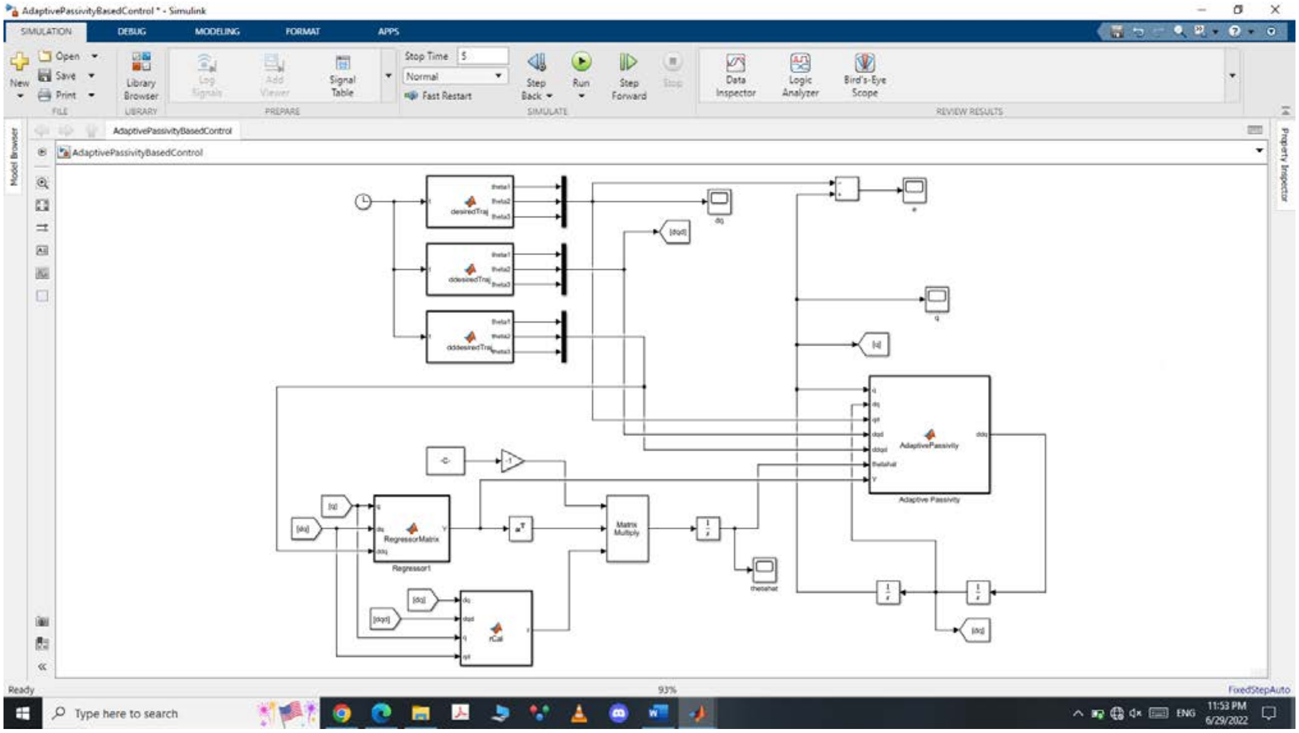

Figure 16- Simulation of adaptive passivity based Controller

According to the simulation, the error is revealed in fig. 17.

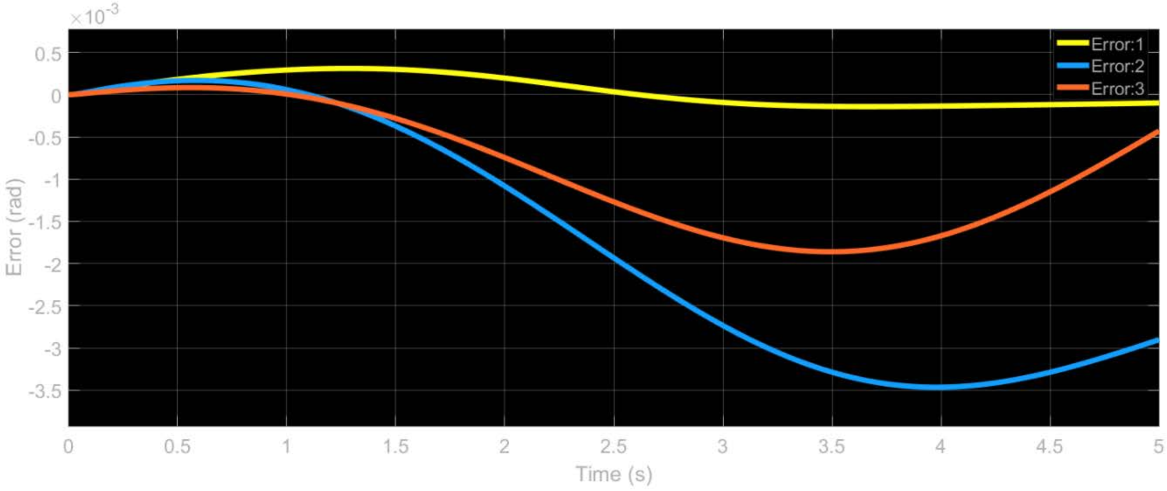

Figure 17- Adaptive passivity based controller simulation results

Impedance Control

The fig. 18 shows the simulations of the controller. The control design assumptions are defined as follows:

```
Cd = [2 1.25 1; -1.25 0.5 0.5; -1 0.5 0];
Kd = [0 0 0; 0 20 0; 0 0 5];
Md = 5.*[3.5 0 0; 0 3.5 0.75; 10 30 15];
```

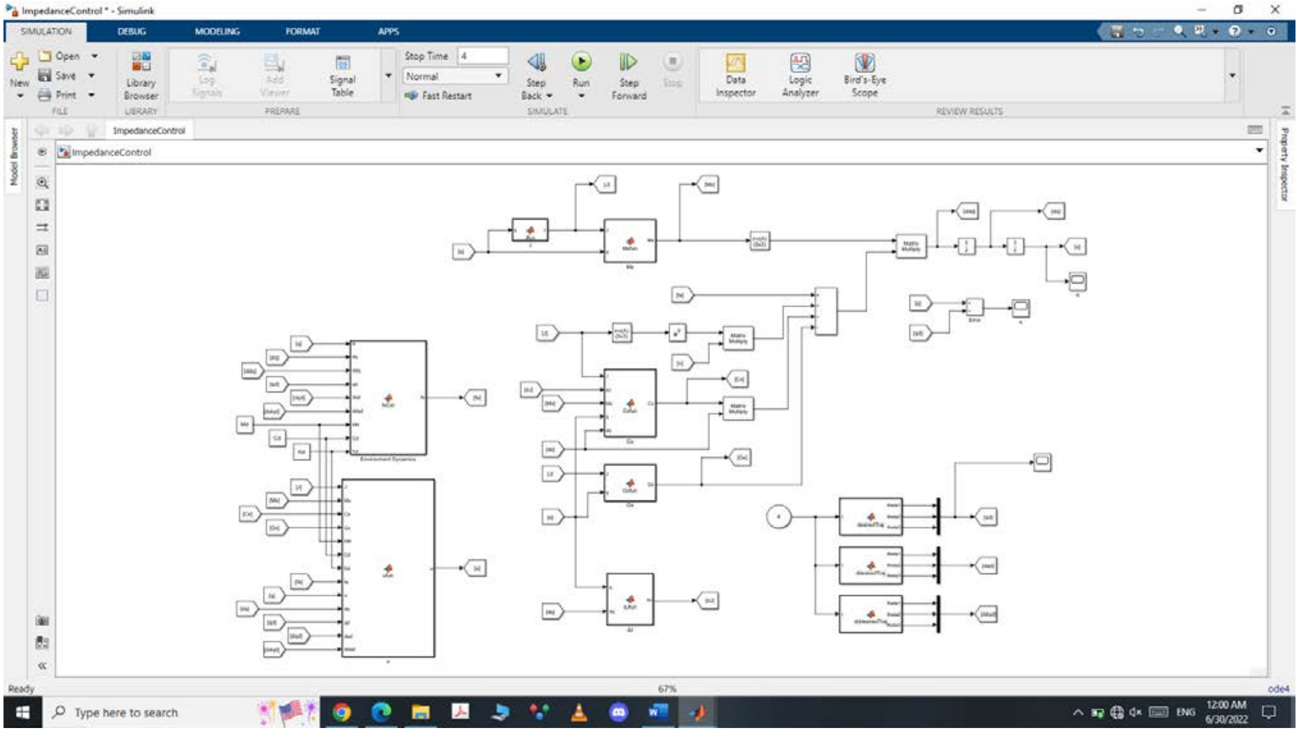

Figure 18- Simulation of impedance Controller

According to the simulation, the error is revealed in fig. 19.

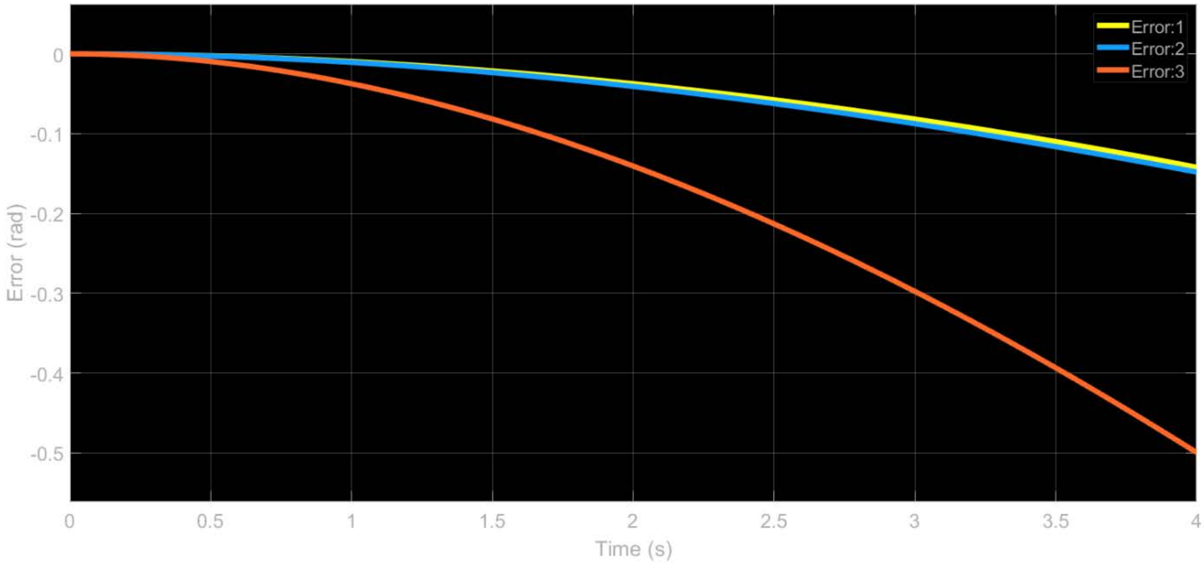

Figure 19- Impedance controller simulation results

Parallel Control

The fig. 20 shows the simulations of the controller. The control design assumptions are defined as follows:

```
Ki = 80.*[1 0 0; 0 1 0; 0 0 10];
Kf = 80.*[1 0 0; 0 1 0; 0 0 1];
Cd = [2 1.25 1; -1.25 0.5 0.5; -3 2 0];
Kd = [0 0 0; 0 20 0; 0 0 50];
Md = 5.*[3.5 0 0; 0 3.5 0.75; 10 30 15];
```

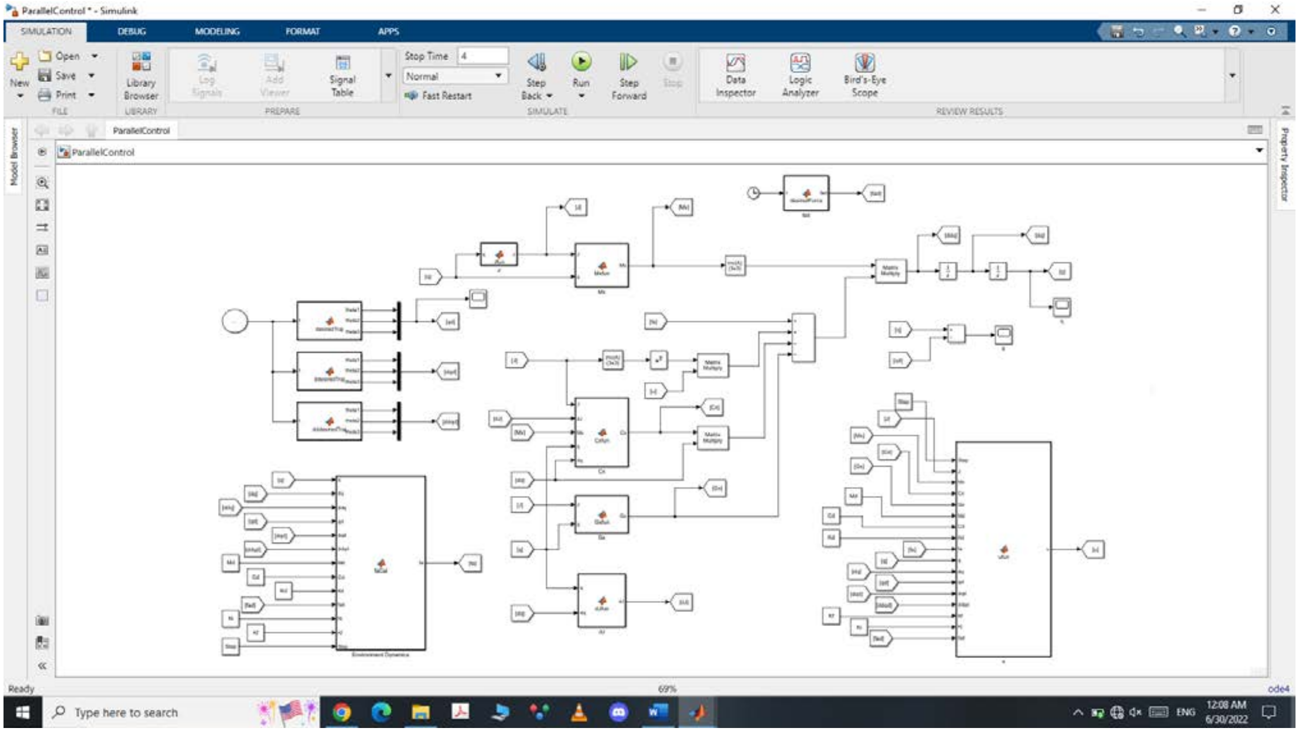

Figure 20- Simulation of parallel Controller

According to the simulation, the error is revealed in fig. 21.

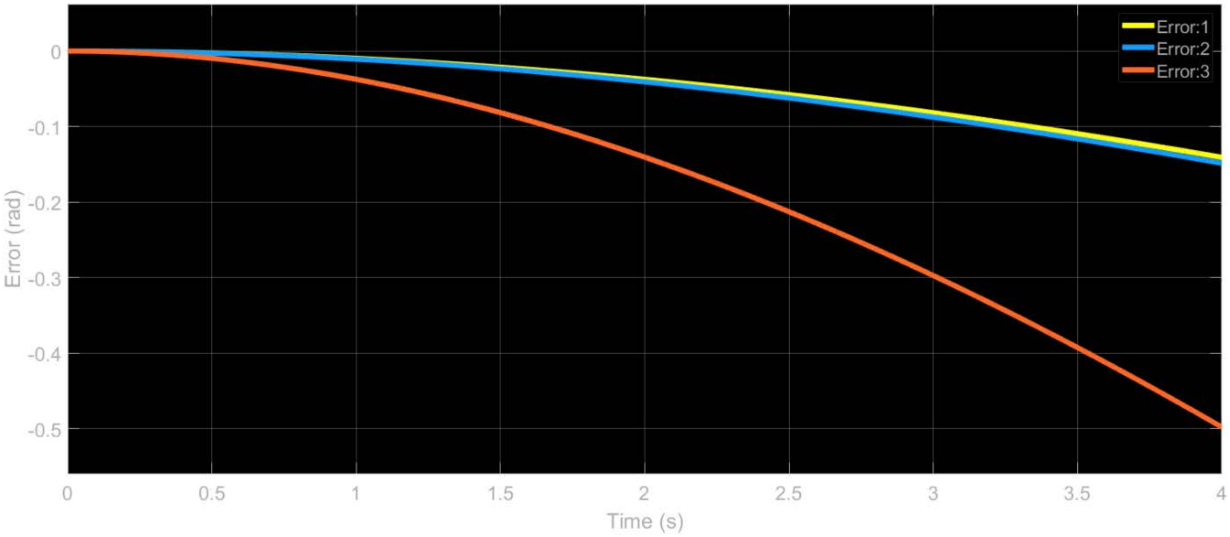

Figure 21- Parallel controller simulation results

Tele-robotics Force-Force Using ISS Approach

The fig. 22 shows the simulations of the controller. The considered system contains two 3-Dof articulated robots one as master and another one as slave. The operator force defined as:

```
Fh = [t; 2*t; 3*t];
```

Also the environment force is defined as:

```
Fe = [0.5*t; 0.6*t; 0.7*t];
```

The delay time between master and slave considered 1 second and parameters of ISS approach are defined as follow:

```
gammaM = [1 0 0; 0 1 0; 0 0 1];
gammaS = [1 0 0; 0 1 0; 0 0 1];
Km = 300.*[1 0 0; 0 1 0; 0 0 1];
Ks = 300.*[1 0 0; 0 1 0; 0 0 1];
```

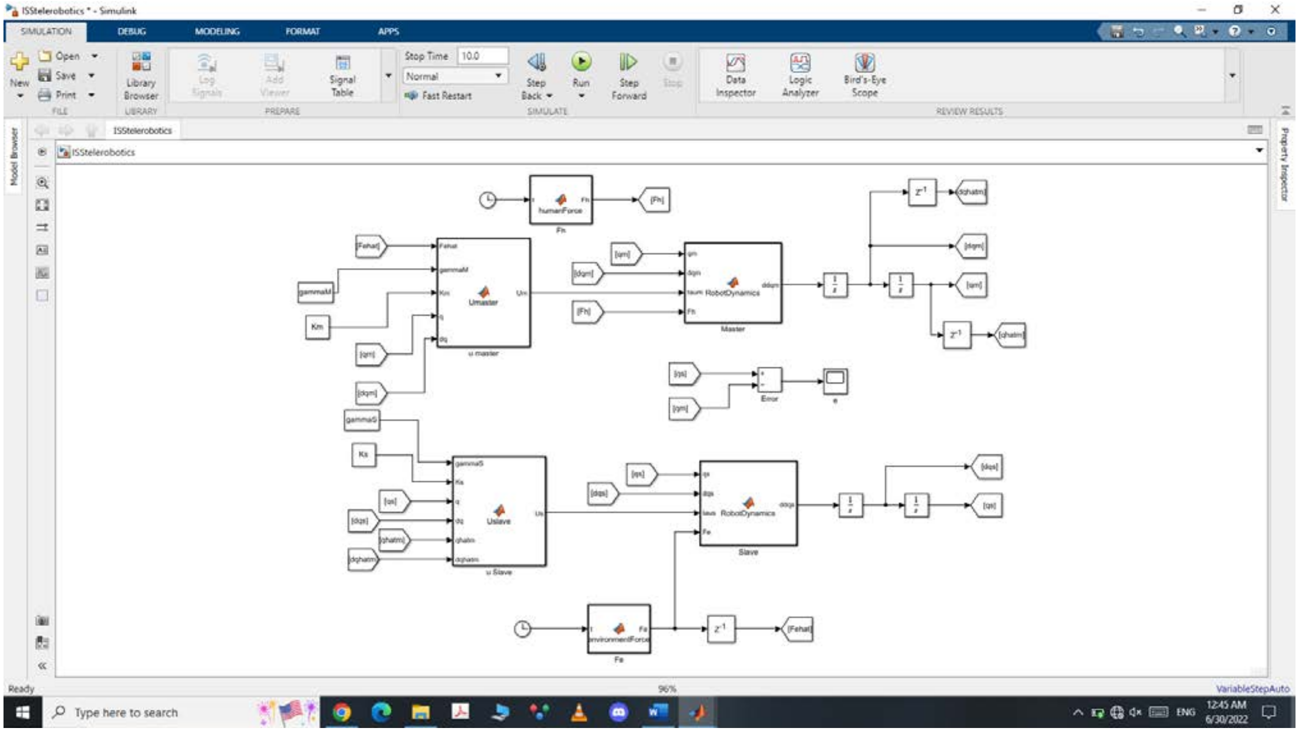

Figure 22- Simulation of tele-robotics system

According to the simulation, the error is revealed in fig. 23.

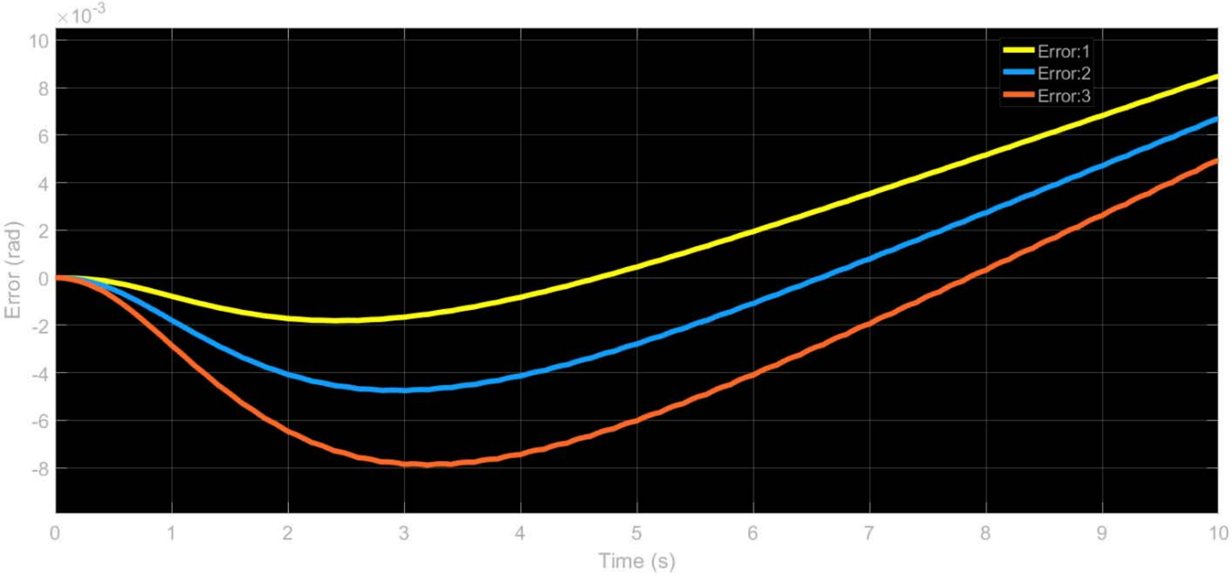

Figure 23- tele-robotics system simulation results